Magnetoresistance hysteresis and critical current density in granular $RuSr_2Gd_{2-x}Ce_xCu_2O_{10-\delta}$

I. Felner,[1,2] E. Galstyan,[2] B. Lorenz,[1] D. Cao,[1] Y. S. Wang,[1] Y. Y. Xue,[1] and C. W. Chu[1,3,4]
[1]*TCSUH and Department of Physics, University of Houston, Houston, Texas 77204-5921*
[2]*The Racah Institute of Physics, The Hebrew University, Jerusalem, 91904 Israel*
[3]*Hong Kong University of Science and Technology, Hong Kong*
[4]*Lawrence Berkeley National Laboratory, Berkeley, California*
(Received 5 September 2002; published 3 April 2003)

We report resistivity data on ceramic $RuSr_2Gd_{2-x}Ce_xCu_2O_{10-\delta}$ which is the first Cu-O based system in which superconductivity (SC) in the CuO_2 planes and weak-ferromagnetism (W-FM) in the Ru sublattice are considered to coexist. Due to the granular nature of the materials the critical current density at 5 K is extremely small as compared to other high-T_C superconducting materials. Below the superconducting transition (T_C), the magnetoresistance $\Delta R(H)=R(H)$-$R(0)$ is positive and unexpected hysteresis loops are observed. The hysteresis loop is completely different than that observed in conventional homogeneous superconductors. $\Delta R(H)$ on decreasing the applied field (H_{ext}) is much smaller than the $\Delta R(H)$ for increasing (H_{ext}). The width of the loops depends strongly on the weak-link properties. Similar hysteresis loops are observed in the reference nonmagnetic $NbSr_2Gd_{1.5}Ce_{0.5}Cu_2O_{10}$ which is SC at $T_C=28$ K, thus the possibility that the hysteresis phenomenom is caused by the coexistence of both SC and magnetic states is excluded.

DOI: 10.1103/PhysRevB.67.134506 PACS number(s): 74.72.Jt, 74.25.Ha, 75.70.Cn

INTRODUCTION

The coexistence of weak-ferromagnetism (WFM) and superconductivity (SC) was discovered a few years ago in $RuSr_2R_{2-x}Ce_xCu_2O_{10}$ (R=Eu and Gd, Ru-1222) layered cuprate systems,[1,2] and more recently[3] in $RuSr_2GdCu_2O_8$ (Ru-1212). The SC charge carriers originate from the CuO_2 planes and the WFM state is confined to the Ru layers. In both systems, the magnetic order does not vanish when SC sets in at T_C, and remains unchanged and coexists with the SC state to within a region of (at least) 10 mm.[3] The Ru-1222 materials (for R=Eu and Gd) display a magnetic transition at $T_M=125-180$ K and bulk SC below $T_C=32-50$ K ($T_M>T_c$) depending on the oxygen concentration and sample preparation.[1] The hole doping of the Cu-O planes, which results in metallic behavior and SC, can be optimized with appropriate variation of the R/Ce ratio.[4,5] SC occurs for Ce contents of 0.4–0.8, and the highest T_C was obtained for Ce=0.6. The isostructural compounds $RuSr_2R_{2-x}Ce_xCu_2O_{10}$ with M=Nb and Ta are also SC below $T_C\sim 28-30$ K, but do not show long-range magnetic order.[6]

The detailed crystal structure and the atomic positions in Ru-1222 were studied by synchrotron x-ray diffraction[7] and neutron diffraction[8] experiments, which show that the RuO_6 octahedra are rotated $\sim$14° around the c-axis and that this rotation is essentially the same for $x=1$ and 0.6, as well as for Ru-1212. There is no evidence for super-cell peaks in the Ru-1222 samples. Specific heat studies of 1222 show a sizable typical jump at T_C and the magnitude of the $\Delta C/T$ (0.08 mJ/gK^2) indicates clearly the presence of bulk SC.[9] The specific heat anomaly is independent of the applied magnetic field. Scanning tunneling spectroscopy,[1] muon-spin rotation[10] and magnetooptic experiments[11] have demonstrated that both states coexist to within the same crystalline grain.

In contrast to the Ru-1212 system in which the antiferromagnetic nature of the Ru sublattice has been determined by neutron diffraction studies,[12,13] the published data up to now have not include any determination of the magnetic structure in Ru-1222. The accumulated results are compatible with two alternative scenarios, both of which are used in understanding the qualitative features at low applied fields. (A) Going from high to low temperatures, the magnetic behavior is basically divided into two regions.[4] (i) Depending on the Ce content, at T_M (which is deduced directly from the temperature dependence M_{sat} and from Mossbauer studies on ^{57}Fe-doped materials), the Ru sublattice becomes antiferromagnetically ordered. (ii) At T_{irr} ($<T_M$), a weak ferromagnetism is detected, which originates from canting of the Ru moments. This canting is probably a result of an antisymmetric exchange coupling of the Dzyaloshinsky-Moriya (DM) type[14] between neighboring Ru moments, induced by the tilting of the RuO_6 octahedra from the crystallographic c axis.[1] This local distortion which breaks the tetragonal symmetry, causes the adjacent spins to cant slightly out of their original direction and to align a component of the moments with the direction of the applied field. At $T_C<T_{irr}$, SC is induced and both SC and WFM states coexist intrinsically on a microscopic scale. (B) A detailed analysis of the magnetization under various thermal-magnetic conditions suggests a phase separation of Ru-1222 into ferromagnetic (FM) and antiferromagnetic[15] (AFM) nanodomains species inside the crystal grains. A minor part of the material becomes FM, whereas the major part orders the AFM part then becomes SC at T_C. In this scenario, the unusual SC state is well understood. However, we will not discuss the magnetic structure further, since it is not essential for the topics concerned in this paper. Neutron diffraction measurements are required to precisely determine the properties of the magnetic order in the Ru-1222 system.

Due to the weakly coupled granular superconductivity of the ceramic Ru-1222 samples, the intrinsic properties of the

SC state are further complicated. The microstructure of Ru-1222 ($x=0.5$) exhibits well-defined grains with a typical size of 1–2 μm and pronounced grain boundaries.[16] The transport transition to the SC state occurs via two intermediate stages.[17] The intragrain sharp drop of the resistivity at T_C occurs when the grains become superconducting. At this point the weak links (WLNs) between the grains contribute a nonzero resistance across the sample. At lower temperature (T_P) the WLNs become superconducting and the intergrain transition is much more sensitive to the magnetic field. The broadening of the resistive transition was already observed in oxygen annealed Ru-1222 materials,[1] and was related to in homogeneity in the oxygen concentration which causes a distribution in WLNs and in the T_C values. In that respect, it is important to resolve these two steps in more detail, in particular the effect of $H_{\rm ext}$ on the magnetoresistance.

In attempting to understand the SC state in the magneto-SC Ru-1222 system, an approach involving systematic investigation of the magnetoresistance below T_C (intragrain) and T_P (intergrain) transitions was employed. For this purpose two batches from the same material have been used, in which the intergrain step was enhanced by exposing the sample to open air. Below T_P, an anomalous magnetic hysteresis in the resistivity is observed, which is more pronounced for the air-exposed sample. This hysteresis, which appears also in SC (nonmagnetic) Nb-1222 sample, is attributed to the granularity of the materials. The theoretical approach[18,19] for granular superconductors which quantitatively explains well this hysteresis is discussed. We start with the low field magnetic measurements on an oxygen annealed Ru-1222 material, which possesses a sharp diamagnetic drop at T_C and a high Meissner fraction.

EXPERIMENTAL DETAILS

Samples of $M{\rm Sr_2Gd_{2-x}Ce_xCu_2O_{10-\delta}}$ ($x=0.6$ and 0.7, $M=$Ru and Nb) were prepared by a solid-state reaction technique as described elsewhere[1,2,15] The as-prepared (asp) $\rm RuSr_2Gd_{1.4}Ce_{0.6}Cu_2O_{10-\delta}$ sample was reheated for a few hours at 600 °C under 300-bar pure oxygen pressure. The dimensions of this bar shaped sample are $0.3\times0.154\times0.08\ {\rm cm}^3$. Part of another as prepared $\rm RuSr_2Gd_{1.3}Ce_{0.7}Cu_2O_{10-\delta}$ sample (kept in a dessicator), was exposed to air at ambient temperature for a few months (denoted as asp and ''air,'' respectively). Determination of the absolute oxygen content in the as prepared materials and in the annealed samples is difficult because CeO_2 is not completely reducible to a stoichiometric oxide when heated to high temperatures. The grain sizes (~3–15 μm) of the ceramic samples were measured using a JEOL JSM 6400 scannung electron microscope.

Zero-field-cooled (ZFC) and field-cooled (FC) dc magnetic measurements in the range of 5–300 K were performed in a commercial (Quantum Design) superconducting quantum interference device (SQUID) magnetometer. The resistance was measured by a standard four contacts probe inserted in the SQUID magnetometer. Powder x-ray diffraction measurements confirmed the purity of the compounds within the instrumental resolution of a few percent, the lattice parameters for all samples are similar to the published data.[1,7,8]

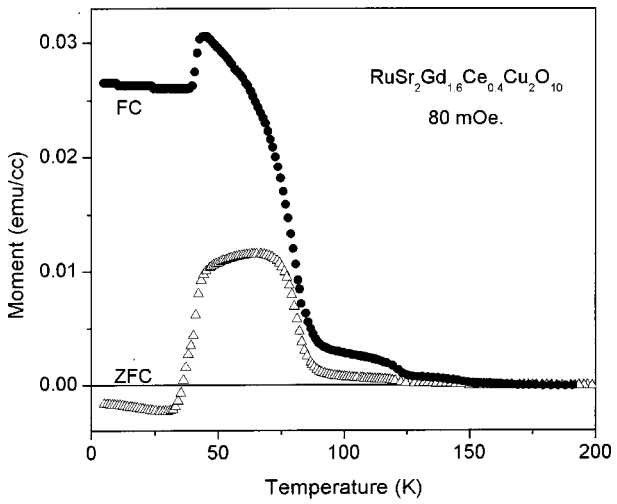

FIG. 1. ZFC and FC susceptibility curves (measured at 80 mOe.) for $\rm RuSr_2Gd_{1.4}Ce_{0.6}Cu_2O_{10}$ as prepared, annealed under 300 oxygen atm. at 600 °C.

EXPERIMENTAL RESULTS

A. Critical current density of Ru-1222

The ZFC and FC curves for the annealed $\rm RuSr_2Gd_{1.4}Ce_{0.6}Cu_2O_{10-\delta}$ sample measured at $H_{\rm ext}=80$ mOe are shown in Fig. 1. The sample was ZFC down to 5 K at nominally zero field, and then a small field ($H_{\rm ext}$) was applied. $H_{\rm ext}=80$ mOe was measured by a calibrated Hall probe inserted into the sample space. The typical expulsion of magnetic flux lines at $T_C=43$ K (confirmed also by four point resistivity measurements) in the FC curve, as well as the flatness below T_C, are readily observed. The $\Delta M_{\rm FC}/H_{\rm ext}$ at T_C is ~70% of 1/4 π value. We have not corrected for the demagnetization factor, which should be small since the sample has a bar-shaped form and $H_{\rm ext}$ is parallel to the long axis.[20]

With the purpose of acquiring information about the transport critical current density (J_C) of this high quality annealed $\rm RuSr_2Gd_{1.4}Ce_{0.6}Cu_2O_{10-\delta}$ sample, we have measured (at 5 K) the I-V curves at various applied fields (Fig. 2). The onset of the resistivity is changed dramatically to lower currents with the applied field below 10 Oe, but is almost unchanged for $H_{\rm ext}$ higher than 20 Oe (not shown). The deduced field dependence of J_C is exhibited in Fig. 3, and the solid line is the fit of curve to $J_C\propto H_{\rm ext}^{-0.045}$. The value obtained at 5 K and $H=0$ (22 A/cm^2) is a few orders of magnitude lower than the measured J_C of ceramic $\rm YBa_2Cu_3O_7$.[21] The intregrain J_C value of Ru-1222 can be evaluated from the remanent moment of the SC Nb-1222 which serves as a reference material, assuming similar SC properties of the two iso-structural systems. The remanent field (at 5 K) obtained for $\rm NbSr_2Gd_{1.4}Ce_{0.6}Cu_2O_{10-\delta}$, is 17.5 Oe. In the Bean model $J_C=30^*\Delta M/d$ (where d is a typical particle size parameter). Taking d as 0.3 cm (the largest dimension in the sample) we obtain $J_C\sim1575$ A/cm^2, a value which is much higher than those in Fig. 3. Therefore, it is

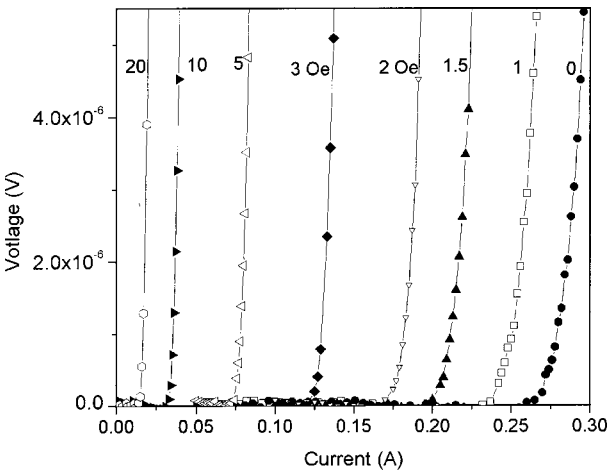

FIG. 2. Current voltage curves at 5 K for annealed $RuSr_2Gd_{1.4}Ce_{0.6}Cu_2O_{10}$ at various applied fields in Oe (marked in the figure).

possible that the low J_C of Ru-1222 is related to its magnetic behavior and more investigation is needed to clarify this point.

B. Weak-link resistance in granular Ru-1222

Figure 4, shows the temperature dependence of resistance of as prepared $RuSr_2Gd_{1.3}Ce_{0.7}Cu_2O_{10-\delta}$ at a fixed current (0.1 mA) at various $H_{\rm ext}$. This behavior is similar to that observed for the Ru-1222 in Ref. 9. It is readily observed that the broad transition for this granular superconductor occurs via two stages. The onset of superconductivity ($T_c = 43$ K) at which the grains become superconducting is not severely affected by $H_{\rm ext}$. A little difference in the onset temperature is observed between 5 and 50 kOe. However, the step-like transition at much lower temperature ($T_P = 38$ K at zero field), which is due to weak-Josephson intergrain coupling, is affected dramatically by the applied field. This is typical for a granular superconductor with weak intergrain

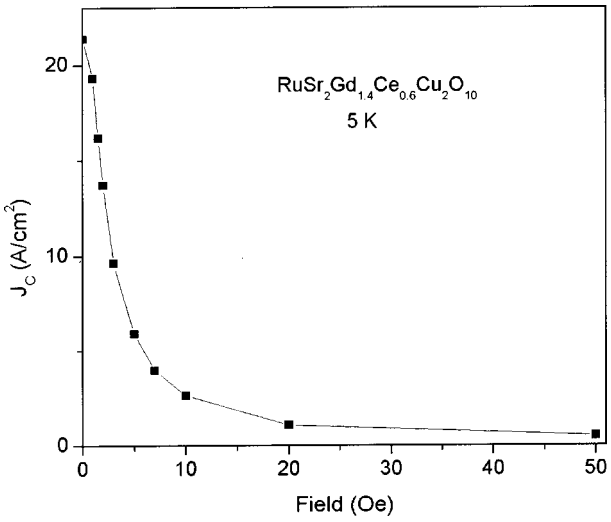

FIG. 3. The field dependence of the critical current density at 5 K.

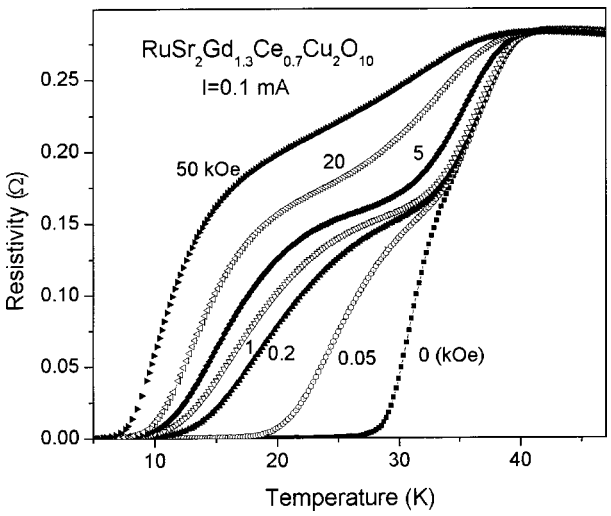

FIG. 4. The temperature dependence of resistivity in magnetic fields up to 50 kOe for $RuSr_2Gd_{1.3}Ce_{0.7}Cu_2O_{10}$.

coupling. The zero resistance temperature decreases rapidly at low fields, and only slowly at high fields. The field dependence of these transitions will be published elsewhere. Generally speaking, below T_P the resistivity is governed mainly by the WLN properties and it is sample dependent. Various parameters affect the WLN properties such as: heat treatment, annealing conditions and the way the samples have been stored prior to measuring.

The isothermal magneto resistance curves (as $H_{\rm ext}$ increases) for temperatures below and above T_P are shown in Fig. 5. Zero resistance is observed even for $H_{\rm ext} = 50$ kOe below 7 K (Fig. 4). At higher temperatures, $R(H) > 0$ at high fields and is strongly dependent on the applied field (up to 0.5–1 kOe), until a common slope is reached. The isothermal $R(H)$ curves are shifted to higher values up to the normal state resistance. Note, that the magneto resistance of the normal state (at 48 K), is negative, similar to that observed in Ref. 9.

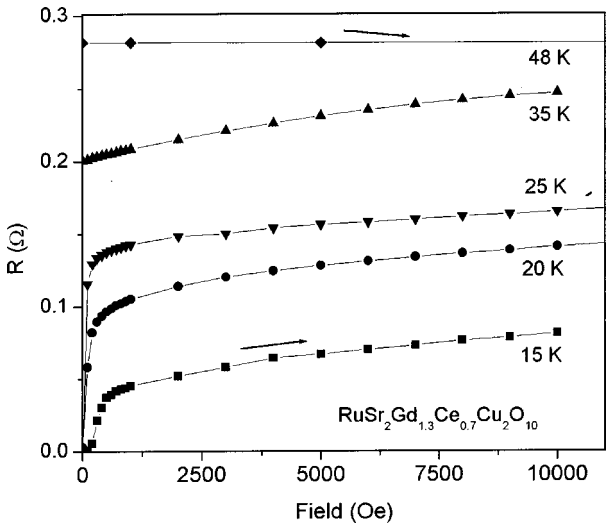

FIG. 5. The magnetic field dependence (for increasing fields) of the resistance of $RuSr_2Gd_{1.3}Ce_{0.7}Cu_2O_{10}$ at various temperatures. The resistivity at 48 K was measured up to 20 kOe.

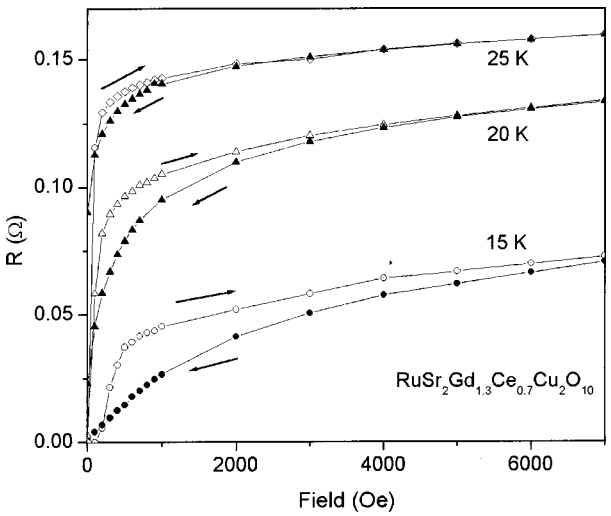

FIG. 6. Hystersis loops of the magnetoresistance of $RuSr_2Gd_{1.3}Ce_{0.7}Cu_2O_{10}$ of at 10, 25, and 25 K; the field directions are signed. The arrows indicate the field direction during the measurement.

Surprisingly, as the applied field is decreased, an anomalous magnetic hysteresis is observed in the magneto resistance curves (Fig. 6). (i) The resistance in the decreasing H_{ext} curve is lower than that in the increasing H_{ext} curve above a crossover field. (ii) Below the crossover field the trend is reversed and at $H_{\text{ext}}=0$ the resistance is finite after the field cycle. The loop's width decreases with temperature and no hysteresis is observed above T_P; thus the hysteresis is the result of the granularity of the material, and depends on the WLN properties. It is also possible that close to T_C, the hysteresis loops are very narrow and thus un-detectable. It should be emphasized that the hysteresis in the magneto resistance curves is neither connected to the magnetic hysteresis loops observed below T_C,[1] nor to the fact that SC and magnetism coexist in these materials. It is interesting to note that the loops' width (ΔH) in Fig. 6 are much larger than the macroscopic demagnetizing field $4\pi M$. For example at 15 K and $H=2000$ Oe, $\Delta H=1400$ Oe, whereas $4\pi M$ is only 360 Oe.

On the other hand, the finite resistance, with decreasing field obtained at $H_{\text{ext}}=0$ and the remanent magnetization moment have the same time response. The relaxation rate of both quantities were measured as follows. At 15 K, a field of 50 kOe was applied and then turned off. The time dependence of the residual resistivity and the remanent magnetization were recorded. The normalized values (i.e., $M(t)-M(\infty)/[M(0)-M(\infty)]$ [where $M(0)$ and $M(\infty)$ are the moments at $t=0$ and 150 min]) are plotted in Fig. 7. The two curves overlap, indicating that the decay of both physical properties have the same origin.

A number of samples with different intergrain properties were investigated to assess the sensitivity of the shape of the magnetoresistance hysteresis loops to variations in the WLNs behavior. Exposing the as prepared $RuSr_2Gd_{1.3}Ce_{0.7}Cu_2O_{10}$ sample to air, reduces T_C from 43 to 40 K and sharply affects the intergrain connectivity. As a result, in contrast to Fig. 4, no zero resistance is obtained at

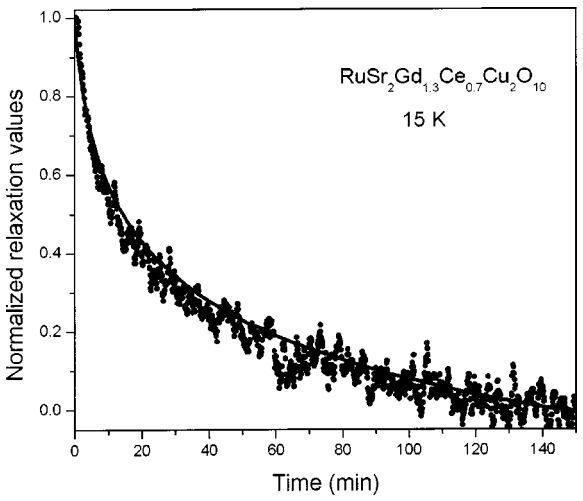

FIG. 7. The time response of the normalized residual resistivity (dots) and the remanent moment (solid line) at 15 K after the withdrawal of a field of 50 kOe.

5 K even for $H_{\text{ext}}=0$ (not shown), and the typical hysteresis in the magnetoresistance is readily observed (Fig. 8). Here again, the resistivity increases with the applied field, and for the descending field the $R(H)$ curve (above a crossover field) is lower than that for the ascending one. In particular, the residual resistance at $H=0$ is nonzero and large when the field is decreased. When the field is ramped from positive to negative and back, the same trend is observed. For the sake of comparison, Fig. 9 displays the hysteresis loops obtained at 15 K for the two: the as prepared and the air exposed samples, which only differ from each other in their WLN properties. In order to compare the loop width of the two materials, the as prepared curve was shifted (by 2.72 Ω) from its original position (see Fig. 6). The magnetic $M(H)$ curves at 15 K and the remanent moment at 5 K are practically the same. Thus the broad loop for the exposed aged sample in Fig. 9 stems only from its poor intergrain connections.

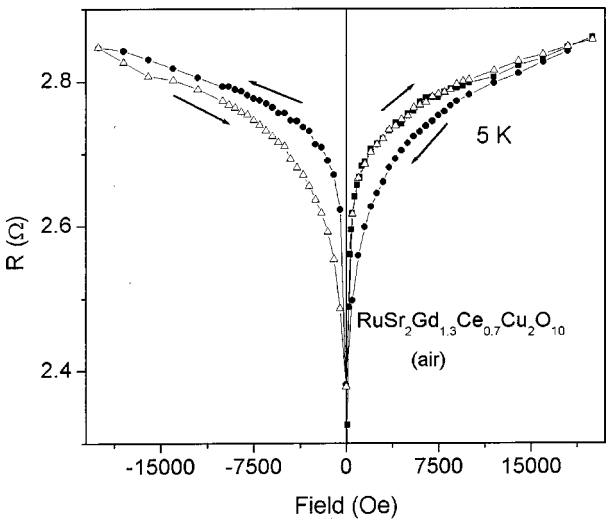

FIG. 8. Hystersis full loops of the magnetoresistance of argon annealed $RuSr_2Gd_{1.3}Ce_{0.7}Cu_2O_{10}$. at 5 K. The field directions are signed by the arrows.

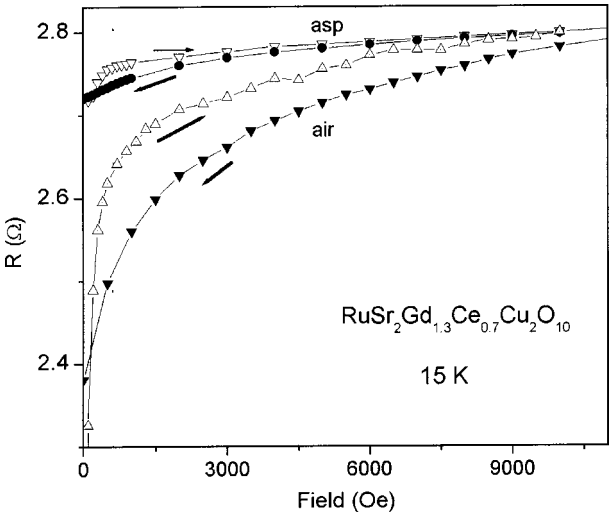

FIG. 9. Magnetoresistance hysteresis loops of as prepared (asp) and air annealed $RuSr_2Gd_{1.3}Ce_{0.7}Cu_2O_{10}$ materials at 15 K. For the sake of clarity, the as prepared curve was shiftted up by 2.72 Ω from its original position. Note the difference in the widths of the two materials.

Similar hysteresis loops have been observed with various $RuSrEu_{2-x}Ce_{x2}Cu_2O_{10}$ samples, and the general trend is that the temperature in which the hysteresis appears as well as the width of loops depend on the heat treatments and annealing procedures of materials. One may propose, that the origin of hysteretic phenomena is the magnetic Ru sublattice which coexists with SC in the Ru-1222 systems. In order to exclude this assumption we measured the temperature dependence of resistance of our reference material, $NbSr_2Gd_{1.5}Ce_{0.5}Cu_2O_{10-\delta}$ at a fixed current (0.1 mA) at various H_{ext} (Fig. 10). This behavior is similar to that observed for the Ru-1222 in Fig. 4. The onset of the intragrain superconductivity ($T_c = 28$ K) is not affected much by H_{ext} whereas $T_P = 22$ K, which is due to weak Josephson intergrain coupling, is affected dramatically by the applied field and shifted to lower temperatures. The zero resistance temperature decreases rapidly at low fields and for $H_{\text{ext}} < 100$ Oe. The resistivity at 5 K is finite. Figure 11 shows the hysteresis loops obtained at 5 and 15 K. Here again, the general trend is that the loops become narrow with temperature, and no hysteresis is observed for $T_P < T < T_C$, similar to the case of Ru-1222 discussed above.

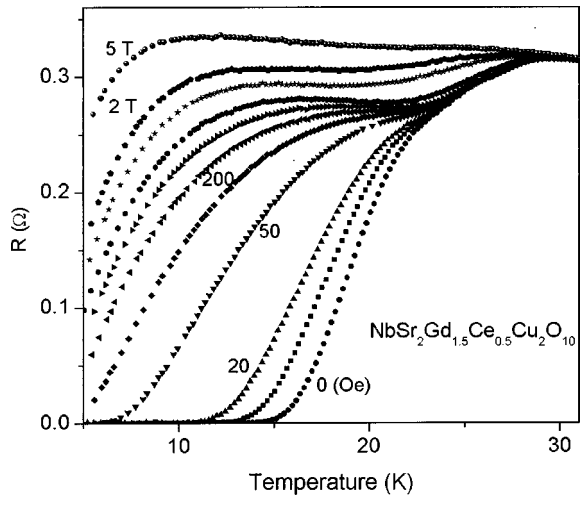

FIG. 10. The temperature dependence of resistivity in magnetic fields up to 50 kOe for $NbSr_2Gd_{1.5}Ce_{0.5}Cu_2O_{10}$. The applied fields are: 0, 10, 20, 50, 100, 200, 500, and 5000 Oe and 1, 2, and 5 T, in sequence as marked for some curves.

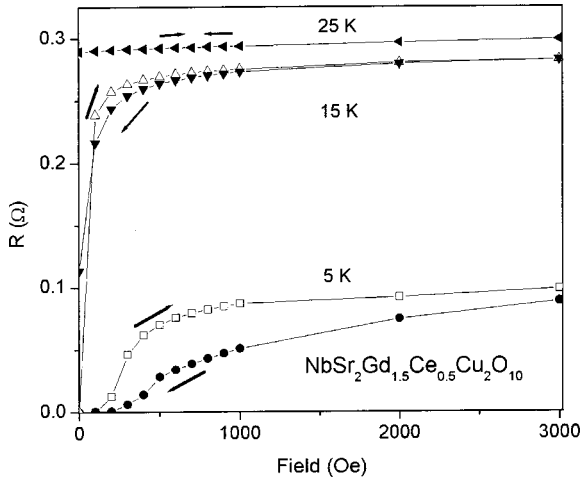

FIG. 11. Hystersis loops of the magnetoresistance of $NbSr_2Gd_{1.5}Ce_{0.5}Cu_2O_{10}$ of at 5, 15, and 25 K. The arrows show the directions of the field change during the measurement.

DISCUSSION

In granular superconducting materials, the non-Ohmic resistivity below T_P is governed by the WLN resistivity which is strongly field dependent (Fig. 5). Qualitatively speaking the hysteresis in the magnetoresistance curves exhibited in Figs. 6, 8, 9, and 11 closely resemble the behavior predicted by the two-level critical-state model of Ji *et al.*[18] They explain qualitatively the surface resistance of granular superconductors, and this model can be extended to describe bulk resistivity as well. For the sake of clarity we will summarize briefly this model.

The conventional critical-state model deals with macroscopically homogeneous superconducting samples, where a single J_C controls the gradient of the flux density everywhere. For granular systems, the two-level critical state model is used and two distinct different current densities are taking place: (i) a large J_C inside the grains, and (ii) a much weaker one reflecting the intergranular Josephson coupling. In other words, two types of fluxons according to their dc pinning characteristics are defined: (a) strong grain-pinned fluxons, and (b) free grain-boundary fluxons which are those that never move through grains. The gradient of the flux density inside the grains is much larger than that in the boundaries between the grains. On a macroscopic scale, the flux density averaged over many grains should have a gradient determined by the weak intergrain properties. The resistivity is dominated by the flux density in the grain boundaries (n_j) due to its smaller pinning strength. n_j is further affected by the combination of the external field H_{ext} and the

field of the local intragrain supercurrents (or the magnetic domains), and experiences an *effective* field of H_{ext}-$\alpha 4\pi M$, where α is a numerical factor. Theoretical calculations of n_j as a function of H_{ext} show that, contrary to homogeneous samples, for the same value of H_{ext}, n_j in the decreasing branch of H_{ext} is *lower* than that in the increasing H_{ext}-branch, except near the remanent state. The explanation for this reduction is as follows. When the field is reduced, some of trapped fluxons are no longer supported by the external field and form closed loops through the grain boundaries. The opposite direction of the flux lines, effectively drives a *reverse* flux component ($-\alpha 4\pi M$) into the sample through the weakest junctions. Because of magnetic field superposition, the average field within the junctions of the weak-links thus becomes ($H_{\text{ext}}-\alpha 4\pi M$) less than the applied field. As a result, J_C in a descending field will be correspondingly increased over the initial J_C curve. Thus the smaller effective field in the grain boundaries leads to the hysteresis observed in Figs. 6, 8, 9, and 11, and this behavior is typical of any granular material. Note the difference in the loop size of the same material but with different grain boundaries (Fig. 9).

This is initially a large effect as the strongest persistent loops in the weak links contribute a large amount of reverse flux. However, as the external field is reduced (or as the temperature is raised) the process of the flux reorganization leads to an increased dispersion of the direction of the local internal field. This will progressively suppress the persistent currents in the weak links by changing the field direction locally at weak links that initially carry a large critical current. Eventually at some $H_{\text{ext}}>0$ the sample will experience a maximum level of cancellation between the applied field and reverse flux, due to remaining flux lines trapped in the grains and as a result, a minimum in the resistivity should be observed.[18,19] This minimum is not observed in our experimental curves, probably because the actual grain size is not uniform and the critical state on the macroscopic level makes the average field vary slightly at different positions in the sample. While this explains qualitatively our experimental results, a more quantitatively theoretical description is needed.

CONCLUSIONS

We have shown that for pure ceramic $RuSr_2Gd_{2-x}Ce_xCu_2O_{10-\delta}$ samples the critical current density in the superconducting state is extremely small. In the superconducting state, the zero-resistance temperature rapidly decreases with the applied magnetic field and depends strongly on the weak-links properties of the materials. Below T_C, the magnetoresistance $\Delta R(H)$ is positive and unexpected hysteresis loops are observed. The $R(H)$ curve for decreasing of the applied field (H_{ext}) is much lower than that of an ascending field. The width of the loops decreases with temperature and varies from sample to sample. Similar hysteresis loops are observed in the reference $NbSr_2Gd_{1.5}Ce_{0.5}Cu_2O_{10}$ which is SC only at $T_C=28$ K. We attribute this behavior to the granular nature of these materials and use the two-level critical-state model to describe it.

ACKNOWLEDGMENTS

This research was supported by the Israel Academy of Science and Technology (2000) and by the Klachky Foundation for Superconductivity. Work at Houston and Berkeley was supported in part by NSF, the State of Texas, DOE, T. L. L. Temple Foundation and J. & R. Endowment. I.F. acknowledges useful conversations with Professor Y. Yeshurun and Professor A. Shaulov at an early stage of this research.

[1] I. Felner, I. Asaf, U. Levi, and O. Millo, Phys. Rev. B **55**, R3374 (1997); I. Felner, U. Asaf, Y. Levi, and O. Millo, Physica C **334**, 141 (2000).

[2] Y. Y. Xue, B. Lorenz, A. Baikalov, D. H. Cao, Z. G. Li, and C. W. Chu, Phys. Rev. B **66**, 014503 (2002); S. Y. Chen *et al.* cond-mat/0105510 (unpublished).

[3] C. Bernhard, J. L. Tallon, Ch. Niedermayer, Th. Blasius, A. Golnik, B. Btucher, R. K. Kremer, D. R. Noakes, C. E. Stronach, and E. J. Ansaldo, Phys. Rev. B **59**, 14 099 (1999).

[4] I. Felner, U. Asaf, and E. Galstyan, Phys. Rev. B **66**, 024503 (2002).

[5] L. Bauernfeind, W. Widder, and H. F. Braun, Physica C **254**, 151 (1995).

[6] R. J. Cava, J. J. Krajewski, H. Takagi, H.W. Zandbergen, R. B. Van Dover, W. F. Peck, Jr., and B. Hessen, Physica C **191**, 237 (1992).

[7] G. V. M. Williams and M. Ryan, Phys. Rev. B **64**, 094515 (2001).

[8] C. S. Knee, B. R. Rainford, and M. T. Weller, J. Mater. Chem. **10**, 2445 (2000).

[9] X. H. Chen, Z. Sun, K. Q. Wang, S. Y. Li, Y. M. Xiong, M. Yu, and L. Z. Cao, Phys. Rev. B **63**, 064506 (2001).

[10] A. Shengelaya *et al.* (unpublished).

[11] S. Y. Chen *et al.*, cond-mat/0105510 (unpublished).

[12] J. W. Lynn, B. Keimer, C. Ulrich, C. Bernhard, and J. L. Tallon, Phys. Rev. B **61**, R14 964 (2000).

[13] J. D. Jorgensen, O. Chmaissem, H. Shaked, S. Short, P. W. Klamut, B. Dabrowski, and J. I. Tallon, Phys. Rev. B **63**, 054440 (2001).

[14] J. Dzyaloshinsky, J. Phys. Chem. Solids **4**, 241 (1958).

[15] Y. Y. Xue, D. H. Cao, B. Lorenz, and C. W. Chu, Phys. Rev. B **65**, 020511(R) (2002).

[16] I. Zivkovic, Y. Hirai, B. H. Frazer, M. Prester, D. Drobac, D. Atiosa, H. Berger, D. Pavuna, G. Margaritondo, I. Felner, and M. Onellion, Phys. Rev. B **65**, 144420 (2002).

[17] Y. Y. Xue, B. Lorenz, R. L. Meng, A. Baikalov, and C. W. Chu, Physica C **364-365**, 251 (2001).

[18] L. Ji, M. S. Rzchowski, N. Anand, and M. Tinkham, Phys. Rev. B **47**, 470 (1993).

[19] J. E. Evetts and B. A. Glowacki, Cryogenics **28**, 641 (1988).

[20] C. Bernard, J. L. Tallon, E. Brucher, and R. K. Kremer, Phys. Rev. B **61**, R14 960 (2000).

[21] I. Felner, B. Brosh, U. Yaron, Y. Yeshurun, and E. Yacoby, Physica C **173**, 337 (1991).